aerospace

MDPI

Article

A Resilient Forward-Looking Terrain Avoidance Warning Method for the Helicopter

Rui Chen [1] and Long Zhao [1,*]

[1] Beijing University of Aeronautics and Astronautics 1, Beijing, 100083, China; ChenRuiBUAA@buaa.edu.cn
* Correspondence: buaa_dnc@buaa.edu.cn.; Tel.: 010-82316764.

Abstract: To solve the nuisance alarm caused by the fixed forward-looking boundary, this paper proposed a resilient forward-looking terrain avoidance method. The method constructed the resilient and adjustable forward-looking boundary model by rolling angle and navigation error, which makes the terrain data perceived by the forward-looking alert closer to the real flight trajectory, reduces the nuisance alarm, and improves the reliability of the alert. The simulation test and verification were carried out using real digital elevation maps and simulated flight data, and compared with the traditional forward-looking terrain avoidance warning method. The simulation results show that the resilient forward-looking terrain avoidance warning method can provide the flight crew with more accurate terrain awareness and improve the reliability of alerts.

Keywords: Helicopter; Terrain Awareness and Warning System; Forward-looking terrain alert

1. Introduction

According to statistics, the vast majority of major aviation fatalities in the world are Controlled Flight Into Terrain (CFIT). CFIT means that the aircraft is in a fully airworthy state, and there is no failure or engine failure of the aircraft itself. The aircraft crashes, falls to the ground or falls into the water, when the flight crew is not aware of the danger, resulting in an aircraft crash or serious damage and casualties [1].

Regarding the CFIT issue, the United States took the lead in launching the Ground Proximity Warning System (GPWS) [2], and in 1976 agreed to authorize the use of GPWS for commercial aircraft. The GPWS system can provide the excessive descent rate warning [3,4], the excessive terrain closure warning [5,6], the negative climb rate after take-off warning [7,8], the unsafe terrain clearance warning [9], the glide slope warning [10] and other mode alarm functions. Each mode receives various flight parameters of the aircraft as input data, and compares these parameters with a variety of internally stored warning thresholds. If any one of the warning thresholds is exceeded, various audible and visual warnings are provided to the crew. The emergence of GPWS significantly improves the safety of aircraft in the take-off stage and approach landing stage, and plays a key role in reducing the occurrence of CFIT [11,12]. In addition, a large number of scholars have improved the warning function of GPWS. For example, literature [13] improved the accuracy of warning judgment by weighted fusion of correction altitudes provided by multiple sensors. Literature [14] generated the terrain clearance floor envelope around the runway, and suppressed the warning within the envelope to avoid excessive interference warnings during landing. For the situation where different mode alarms may occur at the same time, literature [15] proposed a time-based mode switching method. GPWS is a reactive system, and only when the aircraft enters the dangerous area will it give a warning. Therefore, the reaction time reserved by GPWS for pilots is too short, and it lacks prediction ability. The crew can only passively take actions to get rid of the dilemma, and cannot actively avoid the danger.

Citation: Lastname, F.; Lastname, F.; Lastname, F. Title. *Aerospace* **2022**, *9*, x. https://doi.org/10.3390/xxxxx

Academic Editor: Firstname Lastname

Received: date
Accepted: date
Published: date

Publisher's Note: MDPI stays neutral with regard to jurisdictional claims in published maps and institutional affiliations.

Copyright: © 2022 by the authors. Submitted for possible open access publication under the terms and conditions of the Creative Commons Attribution (CC BY) license (https://creativecommons.org/licenses/by/4.0/).

Since the beginning of the 21st century, with the rapid development of digital map technology, navigation technology, and satellite positioning technology, the Enhanced Ground Proximity Warning System (EGPWS) came into being [16]. EGPWS, is also known as Terrain Awareness and Warning System (TAWS) system [17,18]. EGPWS adds Forward Looking Terrain Avoidance (FLTA) and terrain display functions in addition to the original mode alert function. FLTA can provide a "look ahead" function, which not only improves the pilot's awareness of the surrounding terrain situation, but also increases the reaction time before impact. As the core function of the TAWS system, FLTA had received extensive attention from researchers since it was proposed. Literature [19] designed the FLTA envelope by establishing the normal trajectory, vertical trajectory, and inclined recovery trajectory of the helicopter. Literature [20] and [21] designed the vertical envelope of FLTA by establishing the aircraft's standard vertical avoidance maneuver trajectory. Literature [22] studied the time threshold of forward-looking alarm, and analyzed the alarm performance under different time thresholds. Literature [23] proposed a forward-looking warning method that uses terrain matching to correct the relative position error between helicopter and terrain. In addition, for the interference warning, literature [24] proposed a method to adjust the FLTA envelope according to the Required Navigation Performance (RNP) of aircraft.

Although the proposed methods can provide the FLTA function for the crew, the traditional FLTA envelope adopts a trapezoidal side boundary. When the aircraft turns, it is prone to nuisance alarms, which reduces the reliability of the FLTA. To solve this problem, this paper proposes a resilient forward-looking terrain avoidance warning method. The method adjusts the beginning width of the FLTA through the navigation error and terrain resolution. When turning flight, the FLTA side boundary is associated with the roll angle to construct a resilient adjustable side boundary model, which reduces nuisance alarms and improves the reliability of the alerts.

2. Helicopter Terrain Awareness and Warning System (HTAWS)

HTAWS is to evaluate whether the aircraft will crash into the ground through the information provided by airborne sensors such as radio altitude, atmospheric data, attitude, instrument landing, and terrain/obstacle database, and generate corresponding auditory and visual signals. The HTAWS is mainly divided into two types, the mode alert and the FLTA alert. The mode alert mainly uses the current state information of the aircraft provided by the onboard sensor to compare with the known dangerous situation to judge whether to provide an alert. The mode alert includes 6 modes: excessive descent rate warning (Mode 1), excessive terrain closure warning (Mode 2), negative climb rate after take-off warning (Mode 3), unsafe terrain clearance warning (Mode 4), the glide slope warning (Mode 5) and the altitude call and excessive roll/pitch warning (Mode 6) [25].

The principle of FLTA alert is to generate a virtual three-dimensional envelope in the space of the aircraft's forward direction based on the current flight state. When the alert activation conditions (for the helicopter, the activation conditions include that the airspeed is greater than 21m/s, the landing gear status is retracted or the flight height is greater than 3m, and the current altitude is greater than the calculated clipping height) [25] are met, the aircraft automatically obtains data information such as terrain and obstacles, and compares the spatial position relationship between the envelope and the surrounding terrain in real-time. When the surrounding terrain penetrates the envelope, an alert is triggered. The schematic diagram of the FLTA flight is shown in Figure 1. The envelopes for FLTA are divided into caution envelopes and warning envelopes. The design process of the two envelopes is completely the same, and both consist of 4 parts, namely, the look-down boundary, the look-ahead boundary, the look-up boundary and the side boundary. And the difference is that the safety margin of the warning envelope is smaller, and the safety margin of the caution envelope is larger [26]. The specific implementation block diagram is shown in Figure 2.

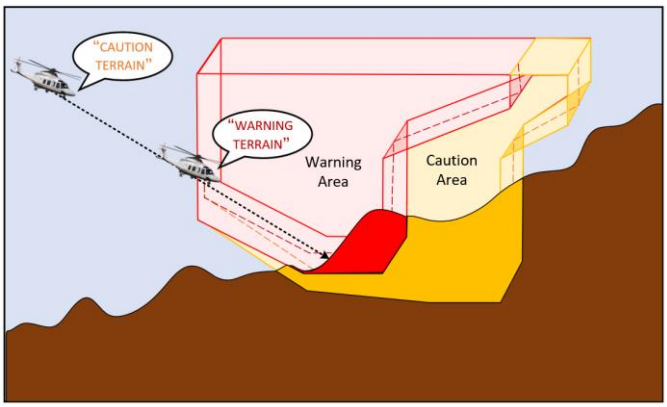


Figure 1. The schematic diagram of FLTA flight.

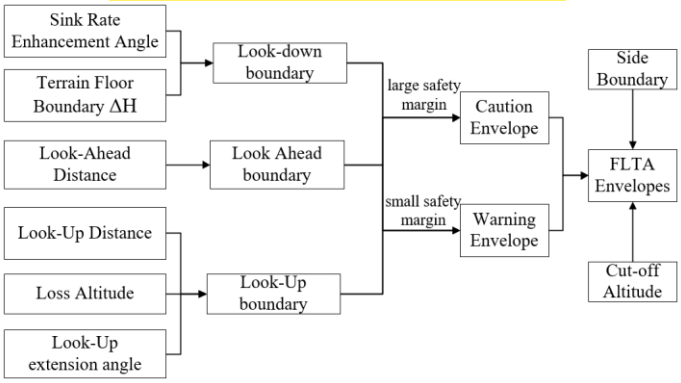


Figure 2. The implementation block diagram.

The look-down boundary is mainly determined by the minimum safe altitude ΔH of the aircraft. During cruise flights, the ΔH is generally set to a fixed value. But during take-off or landing, the ΔH changes with the distance from the aircraft to the nearest runway [26]. To avoid the false alarm when the terrain directly below touches the warning envelope when the aircraft flies over the terrain at a relatively low altitude, a cut-off boundary is set. When the cut-off boundary is larger than the look-down boundary, the cut-off boundary is used as the new look-down boundary. The cut-off boundary starts from the predetermined offset position below the aircraft and extends to the front of the flight at the predetermined cut-off angle. The cut-off angle calculation formula is

$$\theta_{jc} = \min(\gamma, \theta_{sx}) - \delta_b \quad (1)$$

Where γ is the flight path angle. θ_{sx} is the upper limit of the cut-off angle. δ_b is the base value.

The look-ahead boundary is determined by the look-ahead distance and the corresponding influence coefficient. For the helicopter, the look-ahead distance is equal to the sum of the reaction distance and the distance from cruise to hover. The look-ahead distance calculation formula is

$$D_{LA} = \frac{V^2}{2g \tan \alpha} + V \cdot T \quad (2)$$

Where V is the flight speed. g is the gravitational acceleration. α is the nominal pitch angle for hovering. T is the reaction time of the pilot.

The look-up boundary is determined by the loss altitude, the look-up distance and the look-up extended angle. The look-up distance is equal to the look-ahead distance multiplied by the different coefficients. To avoid threatening terrain, the aircraft needs to do the maneuver of pulling up and climbing. The descending height from the beginning of the maneuver to the climb is the loss altitude, and the calculation model is

$$\begin{cases} dH_c = \dfrac{3}{4}\Delta H + V_z \times T_1 + \dfrac{V_z^2}{2a} \\ dH_w = \dfrac{1}{2}\Delta H + \dfrac{V_z^2}{2a} \end{cases} \tag{3}$$

Where dH_c represents the loss altitude of the caution alert. And the dH_w represents the loss altitude of the warning alert. V_z is the vertical speed. a is the acceleration during the pull-up maneuver.

The side boundary is mainly composed of the beginning width B_w, the centerline deflection angle θ and the side deviation angle δ, as shown in Figure 3. The centerline of the side boundary starts from the current position of the aircraft and extends to both sides with a fixed deviation angle to form a trapezoidal side boundary. The trapezoidal side boundary can better perceive the terrain in front of the aircraft when flying in a straight line. When the aircraft turning, the accuracy of terrain awareness will be reduced.

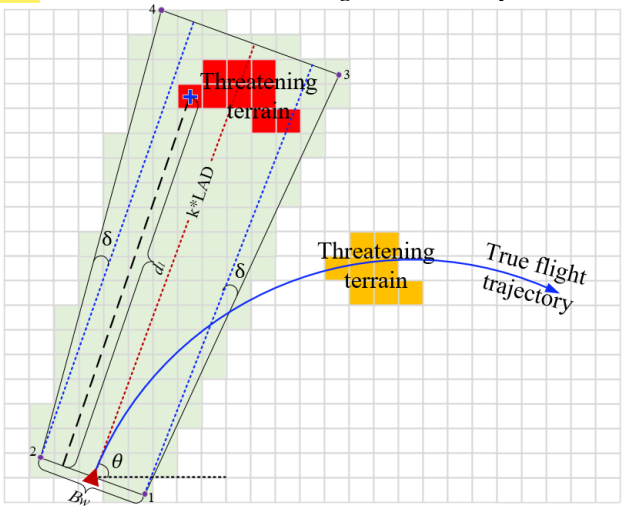


Figure 3. Trapezoidal side boundary.

The design process of the trapezoidal side boundary and the extraction of terrain data within the side boundary consists of the following 5 steps.

(1) According to the current position (c_0, r_0) of the aircraft, the row and column coordinates of the four endpoints of the trapezoidal boundary on the digital terrain elevation map is calculated as

$$\begin{cases} r_1 = r_0 + 1/2 * B_w * \cos(\theta) \\ r_2 = r_0 - 1/2 * B_w * \cos(\theta) \\ r_3 = r_1 - k_3 * D_{LA} / \cos(\delta) * \sin(\theta - \delta) \\ r_4 = r_2 - k_3 * D_{LA} / \cos(\delta) * \sin(\theta + \delta) \end{cases} \tag{4}$$

$$\begin{cases} c_1 = c_0 + 1/2 * B_w * \sin(\theta) \\ c_2 = c_0 - 1/2 * B_w * \sin(\theta) \\ c_3 = c_1 + k_3 * D_{LA} / \cos(\delta) * \cos(\theta - \delta) \\ c_4 = c_2 + k_3 * D_{LA} / \cos(\delta) * \cos(\theta + \delta) \end{cases} \tag{5}$$

Where D_{LA} is the look-ahead distance. k_3 is the coefficient of the caution look-up distance.

(2) Construct a polygon database from vertex coordinates. And store the maximum ordinate R_{max}, starting abscissa C_{max} and reciprocal of slope k corresponding to each line segment.

(3) Arrange the coordinate data of the sampling points stored in (2) in ascending order. Using the scan line method, the terrain between the line segments is retrieved and stored.

(4) For each terrain data retrieved, calculate the distance dl from the beginning width Bw. Then, arrange dl in ascending order, and split the retrieved terrain data according to the set distance threshold.

(5) For the forward-looking alert, an alert is issued as long as there is a high terrain penetration boundary. Therefore, the maximum value of each row in the split terrain data is compared with the envelope to realize a forward-looking alert judgment.

Through digital map technology, FLTA can obtain the terrain in front of the flight, and compare it with the real-time calculated three-dimensional alert envelope to warn the dangerous terrain in front in advance. It not only increases the flight crew's perception of the surrounding terrain but also facilitates the crew to adopt a gentler avoidance strategy. However, the FLTA alert relies on the envelope and the extracted terrain elevation information. When the aircraft maneuvers and turns, the traditional trapezoidal side boundary centerline gradually deviates from the real flight trajectory with the increase of the foresight distance. It can be seen in Figure 3, the red threat terrain not in front of the flight will lead to the false alarm. And the yellow threat terrain in front of the real flight will cause the missing alarm. These interference alarms will affect the normal flight of the crew and reduce the reliability of the FLTA alert.

3. Resilience forward-looking terrain avoidance warning method (RFLTA)

The resilience forward-looking terrain avoidance warning method retains the look-down boundary, the look-ahead boundary and the look-up boundary in the traditional method, and mainly optimizes the side boundary. The method combines the current map resolution and 3 times the real-time estimation error of the navigation system to design the beginning width. And the forward-looking alert envelope is resiliently adjusted according to the aircraft roll angle. When the aircraft is flying in a straight line, the trapezoidal side boundary is used to extract the terrain data within the envelope, and when the aircraft is turning, the terrain data is extracted using the pipe-shaped side boundary. The schematic diagram of the pipe-shaped side boundary is shown in Figure 4, where the square represents the terrain grid, the green square represents terrain elevation extracted from the side boundary, and the red and yellow squares represent the threat terrain.

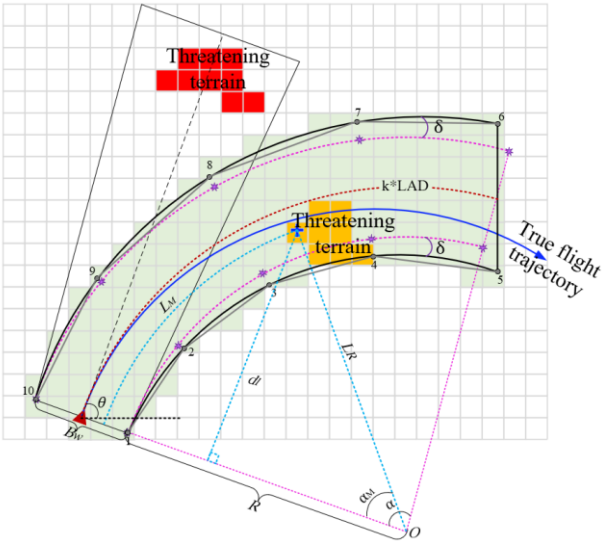


Figure 4. The pipe-shaped side boundary.

The design process of the pipe-shaped side boundary and the extraction of terrain data within the side boundary consists of the following 7 steps.

(1) According to the real-time estimation error σ_{xy} provided by the aircraft navigation system and the resolution *res* of the map data currently used by the aircraft, adjust the beginning width B_w of the boundary as

$$Bw = 3*\sigma_{xy} + res \tag{6}$$

(2) According to the current position of the aircraft (c_0, r_0), speed V, attitude and other information, calculate the radius R of the pipe-shaped boundary, the coordinates of the center of the circle (x_o, y_o), the Center Angle α and the coordinates of the baseline endpoints (c_s, r_s), (c_e, r_e).

$$R = \frac{V^2}{g\tan\gamma} \tag{7}$$

$$\begin{cases} x_o = c_0 + R\sin(\theta) \\ y_o = r_0 + R\cos(\theta) \end{cases} \tag{8}$$

$$\alpha = \frac{k_3 D_{LA} * 180}{\pi R} \tag{9}$$

$$\begin{cases} r_s = r_0 + 0.5 * B_w \cos(\theta) \\ r_e = r_0 - 0.5 * B_w \cos(\theta) \end{cases} \tag{10}$$

$$\begin{cases} c_s = c_0 + 0.5 * B_w \sin(\theta) \\ c_e = c_0 - 0.5 * B_w \sin(\theta) \end{cases} \tag{11}$$

Where, γ is the aircraft roll angle. θ is the angle between the centerline and the east.

(3) Set the sampling number *S*. Sampling the equal central angle of the pipe-shaped boundary to obtain the coordinates of the sampling point on the arc. And take the endpoint of the baseline as the fixed point, expand the sampling point according to the set deviation angle δ, and obtain the coordinates of the sampling point after the deviation.

$$\begin{cases} c(i) = c_j + (c_i - c_j)\cos(\delta) - (r_i - r_j)\sin(\delta) \\ r(i) = r_j + (c_i - c_j)\sin(\delta) + (r_i - r_j)\cos(\delta) \end{cases} \tag{12}$$

Where *i* represents the *i-th* sampling point. (c_i, r_i) represent the coordinates of both ends of the initial width respectively, *j=s* represents the starting endpoint, and *j=e* represents the ending endpoint.

(4) Connect each sampling point end to end to construct a pipeline-shaped approximate polygon. A polygon database is constructed to store the maximum ordinate R_{max}, the initial abscissa C_{max} and the reciprocal of the slope *k* corresponding to each line segment.

(5) Arrange the coordinate data of the sampling points stored in (2) in ascending order. Using the scan line method, the terrain between the line segments is retrieved and stored.

(6) For each terrain data retrieved, calculate the distance *dl* from the starting width *Bw* and the distance L_R from the center of the circle. Then, the corresponding central angle α and arc length L_M are obtained. Arrange L_M in ascending order, and split the retrieved terrain data according to the set distance threshold.

(7) For the forward-looking alert, an alert is issued as long as there is a high terrain penetration boundary. Therefore, the maximum value of each row in the split terrain data is compared with the envelope to realize a forward-looking alert judgment.

4. Experimental results and analysis

The resilient forward-looking terrain avoidance warning method is tested and verified by using real terrain elevation data and simulated flight trajectory. The size of the digital terrain elevation map used in the experiment is 540km×540km, and the map resolution is 30m. The terrain contour map and the three-dimensional simulated flight trajectory are shown in Figure 5 and Figure 6, respectively. The initial height of the simulated flight trajectory is 518.16m. The initial speed is 25.72m/s. The width of the safety corridor caused by the navigation and positioning error is 90m. The updated frequency of the flight status data is 50Hz.

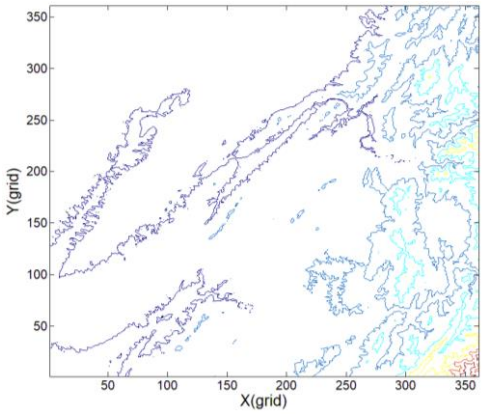


Figure 5. The terrain contour map.

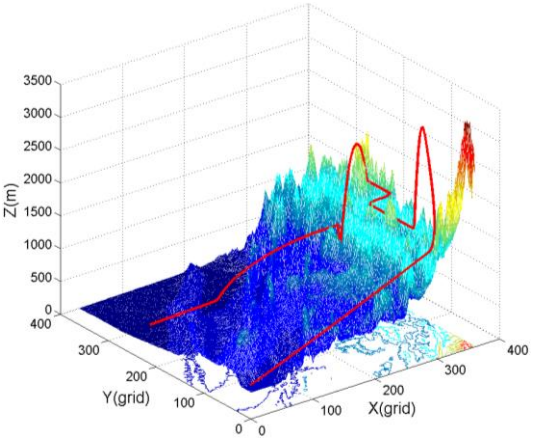


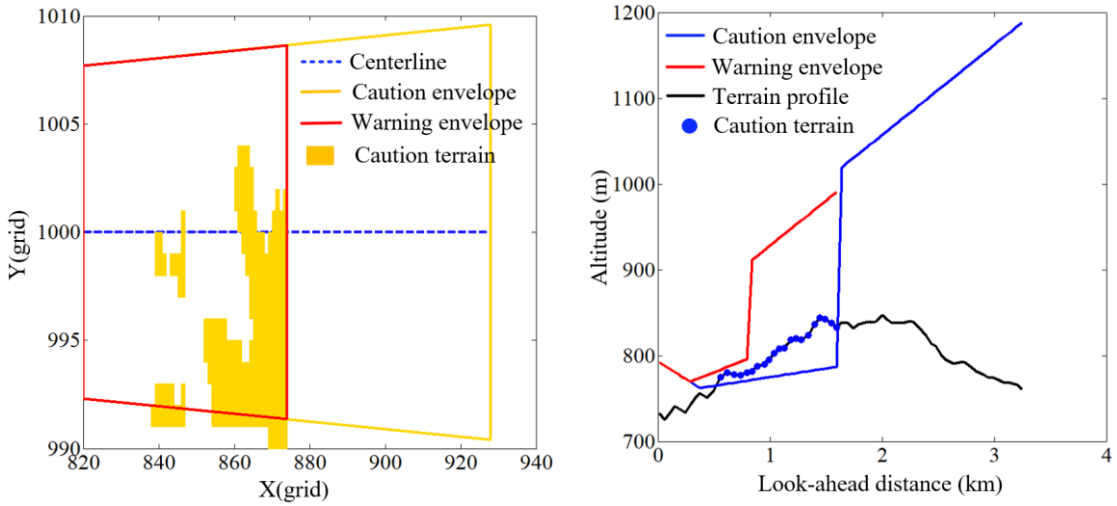
Figure 6. 3D terrain and simulation trajectory.

The RFLTA caution and warning alert tests are carried out in the direct flight situation and the turn situation, respectively. The roll angle, forward-looking distance (DLA), radio altitude and remaining impact time are counted as shown in Table 1. The RFLTA caution alert and warning alert results are shown in Figure 7 and Figure 8.

Table 1. The RFLTA alert results under different alert types.

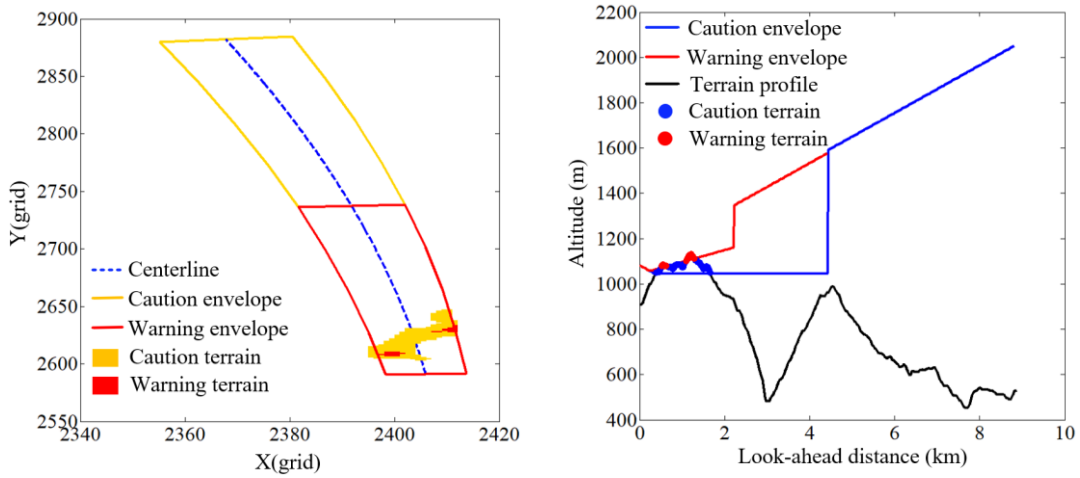
Alert Type	Roll angle	D_{LA}	Radio altitude	Remaining impact time
Caution Terrain	0°	1.62km	101m	10.46s
Warning Terrain	6.32°	2.35km	225m	5.86s

As can be seen from Figure 7 and Figure 8, when the threatening terrain ahead of the flight penetrates the caution envelope, the system can give a voice of "Caution Terrain". When the threatening terrain ahead of the flight penetrates the warning envelope, the system can give a voice of "Warning Terrain". In addition, different from the mode alert, when the alert occurs, the method can calculate the remaining impact time based on the current flight state parameters for the flight crew's reference. As shown in Table 1, for the caution alert shown in Figure 7, the remaining time for the aircraft to hit the nearest threatening terrain is 10.46s. And for the warning alert shown in Figure 8, the aircraft is close to the threatening terrain, and the remaining impact time is 5.86s.



(**a**) (**b**)

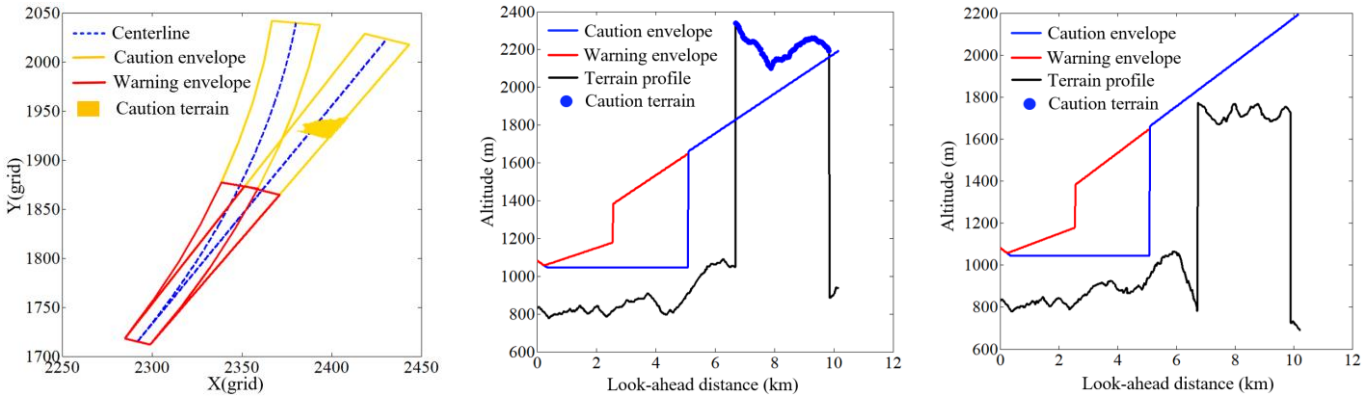
Figure 7. RFLTA Caution alert results. (**a**) Horizontal result; (**b**) Vertical result.



(**a**) (**b**)

Figure 8. RFLTA Warning alert results. (**a**) Horizontal result; (**b**) Vertical result.

To further test the performance of the RFLTA method, under the same turning flight, the traditional alert envelope and the resilient alert envelope are used to experiment respectively, and the experimental results are shown in Figure 9. The horizontal boundaries of the two methods are drawn on the horizontal flight trajectory curve, and the terrain elevations extracted by the two methods are compared with the terrain elevations under the real trajectory, as shown in Figure 10 and Figure 11, respectively. For the turning flight in the simulated flight trajectory, we count the interference alarm and the elevation difference with the real terrain profile under two methods, as shown in Table 2. The interference alarm mainly includes false alarm N_F and missing alarm N_M. If the terrain profile below the real trajectory does not penetrate the alert boundary, and the extracted terrain profile penetrates the alert boundary, it is recorded as a false alarm. On the contrary, if the terrain profile below the real trajectory penetrates the warning boundary, and the extracted terrain profile does not penetrate the alert boundary, it is recorded as a missing alarm. The terrain profile information mainly calculates the mean H_M and standard deviation H_S of the elevation difference between the extracted terrain profile and the real terrain profile.



(**a**) (**b**) (**c**)

Figure 9. Comparison results of the two methods. (**a**) Horizontal alert; (**b**) Traditional method Vertical alert; (**c**) RFLTA method Vertical alert.

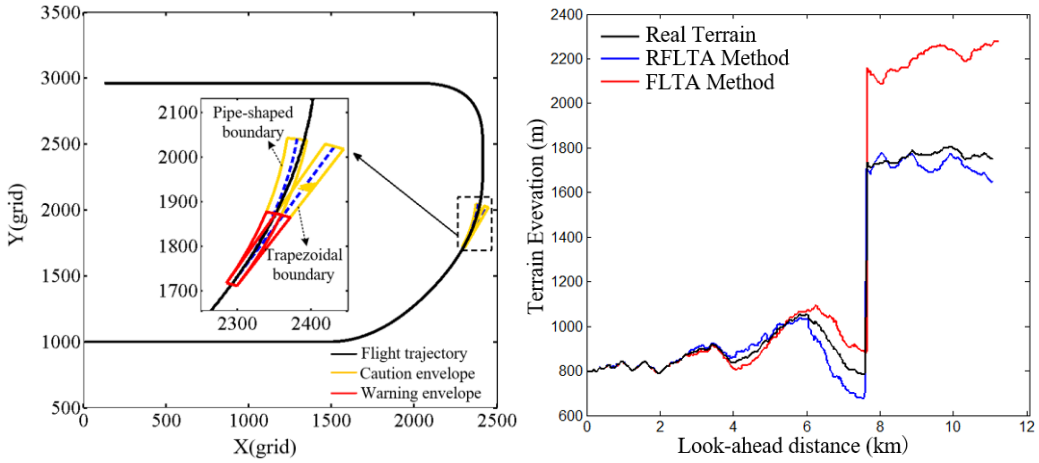


Figure 10. Two boundaries on the horizontal flight curve. **Figure 11.** Terrain curves comparison.

Table 2. The alert results under two methods in turning flight.

	Total epoch	N_R*	**Boundary type**	N_T*	N_C*	N_F	N_M	H_m(m)	H_s(m)
First turning	471	0	Trapezoid	12	0	12	0	-10.4	35.8
			Pipe	0	0	0	0	-2.1	29.9
Second turning	251	64	Trapezoid	132	43	89	21	-103.9	125.4
			Pipe	65	62	3	2	13.1	37.6

*Note: N_R represents the number of real alerts. N_T represents the total alerts under different methods. N_C represents the number of correct alerts.

It can be seen from Figure 9 to Figure 11 that the traditional FLTA method has a caution alert, while the RFLTA method does not generate an alert. From the terrain elevation curve directly below the real flight trajectory, it can be seen that the terrain elevation extracted by the RFLTA method is closer than the traditional FLTA method. And there is no threatening terrain ahead, so it can be judged that the traditional FLTA method has occurred false alarm. And compared to the trapezoidal boundary, the pipe-shaped side boundary is closer to the trajectory of the aircraft when it turns. Table 2 summarizes the alarms under two turning flights. From the number of false alarms and missing alarms, it can be seen that compared with the traditional trapezoidal boundary, the number of false

alarms and missing alarms of the pipe-shaped boundary proposed in this paper is significantly reduced. Moreover, from the difference between the extracted terrain profile and the real terrain profile, we can also see that the difference of the proposed method is smaller, the awareness terrain is more accurate, and can effectively improve the reliability of the HTAWS.

5. Conclusions

This paper proposed a resilient forward-looking terrain avoidance method. The RFLTA method adjusts the forward-looking boundary according to the navigation error and roll angle of the aircraft. The designed pipe-shaped side boundary can reduce the interference alarms under turning flight, and enhance the pilot's ability to perceive the terrain ahead. The actual digital terrain elevation map and simulated flight data are used for testing and verification. Compared with the traditional FLTA method, the terrain profile extracted by the RFLTA method is closer to the real profile, and the number of false alarms and missing alarms are significantly reduced. Although the RFLTA method can improve the reliability of the TAWS, it can not guarantee flight safety. How to avoid threatening terrain entirely depends on the pilot's own experience. Therefore, future work will focus on giving safe avoidance suggestions.

Author Contributions: writing—original draft preparation, Rui.Chen.; writing—review and editing, Long.Zhao. All authors have read and agreed to the published version of the manuscript.

Funding: The project was funded by the National key research and development program of China (Grant No. 2020YFB0505804), the National Natural Science Foundation of China (Grant No. 41874034), and the Natural Science Foundation of Beijing (Grant No. 4202041).

Data Availability Statement: Not applicable.

Conflicts of Interest: The authors declare no conflict of interest.

References

1. International Civil Aviation Organization. Controlled Flight into Terrain: Education and Training Aid. Technical Report January, International Civil Aviation Organization, 2005.
2. Astengo R. A.. Ground Proximity Warning System Utilizing Radio and Barometric Altimeter Combination. FR2102182, 1977.1.21.
3. Bateman C. D.. Excessive descent rate warning system for aircraft. CA1058306, 1979.7.10.
4. Bateman C. D.. Aircraft excessive descent rate warning system. US4215334,1980.7.29.
5. Brem F. J, Muller H. R., Bateman C. D.. Terrain closure warning system with climb inhibit and altitude gain measurement. CA1039535,1978.10.03.
6. Muller H. R., Bateman C. D.. Terrain closure warning system with altitude rate signal conditioning. CA1071740, 1980.2.12.
7. Bateman C. D., Muller H. R.. Negative climb rate after take-off warning system with predetermined loss of altitude inhibit. CA1058305, 1979.7.10.
8. Paterson N. S., Vermilion E. E.. Negative climb after take-off warning system. US4951047, 1990.8.21.
9. Bateman C. D.. Terrain clearance warning system for aircraft. CA1128627, 1982.7.27.
10. Muller H. R., Bateman C. D.. Glide slope warning system with a variable warning rate. CA1070803, 1980.1.29.
11. Xiao W., Zhu X., Zhou Z.. An automatic ground test method for the analogue unit of Ground Proximity Warning System. Quality Reliability Risk Maintenance and Safety Engineering International Confe, 2011, pp.281 - 283.
12. Michael C.. Dorneich P. M., Michael D. G.. Design and Evaluation of an Integrated Avionics Alerting System. The 20th Digital Avionics Systems Conference. Daytona Beach, 2001, pp. 14-18.
13. Johnson S. C., Muller H. R.. Method and apparatus for determining altitude. EP1058816, 2004.4.7.
14. Ishihara Y., Gremmert S., Johnson C.. Apparatus, method, and computer program product for generating terrain clearance floor envelopes about a selected runway. DE60011996, 2005.7.21.
15. Bateman C. D.. Ground proximity warning system with time based mode switching. CA1177562, 1984.11.6.
16. Breen B.C.. Controlled Flight Into Terrain and the enhanced Ground Proximity Warning system. IEEE Aerospace and Electronic Systems, 2002, Vol.14, No.1, pp.19-24.
17. Josel S.. Development of the Forward Looking Terrain Avoidance in a Terrain Awareness and Warning System (TAWS). Graz University of Technology, 2012.
18. Gang X., Fang H., Wu J.. Research on an EGPWS/TAWS simulator with forward-looking alerting function. IEEE/AIAA 33rd Digital Avionics Systems Conference (DASC), 2014, pp. 7D4-1-7D4-11.

19. Zhou Y., Zhou C. Z., Chen G. Y.. A helicopter forward-looking terrain warning method. CN105844972B, 2018.5.18.
20. Dong S., Li W J., Zhou Y H.. Modeling and simulation of Enhanced Ground Proximity Warning System. The 2nd International Symposium on Systems and Control in Aerospace and Astronautics, 2008, pp. 1-4.
21. Fu Y., Zhao X. D.. Simulation Research and Design of Flight Simulator Enhanced Ground Proximity Warning System. Measurement and Control Technology, 2021, Vol. 40, No.5, pp.101-104.
22. Zhang H M., Yang C.. Forward-looking Alerting Threshold Analysis of TAWS Based on Probability Methods. Journal of System Simulation, 2013, Vol.25, No.3, pp.253-259.
23. Zhang S Y., Lu Y.. Helicopter forward looking alert method for low-altitude flight based on terrain matching. Journal of Beijing University of Aeronautics and Astronautics, 2019, Vol.45, No.2, pp.340-346.
24. Johnson S. C., Ishihara Y.. System for monitoring RNP for safe terrain clearance. EP1857781, 2010.4.14.
25. Peter Clapp, David Howson. Report for UK Civil Aviation Authority on Class A Terrain Awareness Warning System (TAWS) for Offshore Helicopter Operations[Z]. UK CAA, 2017.
26. Anderson T., Jones W., Beamon K.. Design and implementation of TAWS for rotary wing aircraft. Aerospace Conference, 2011, pp.1-7.